Figure S1. Syrovatkina et al.

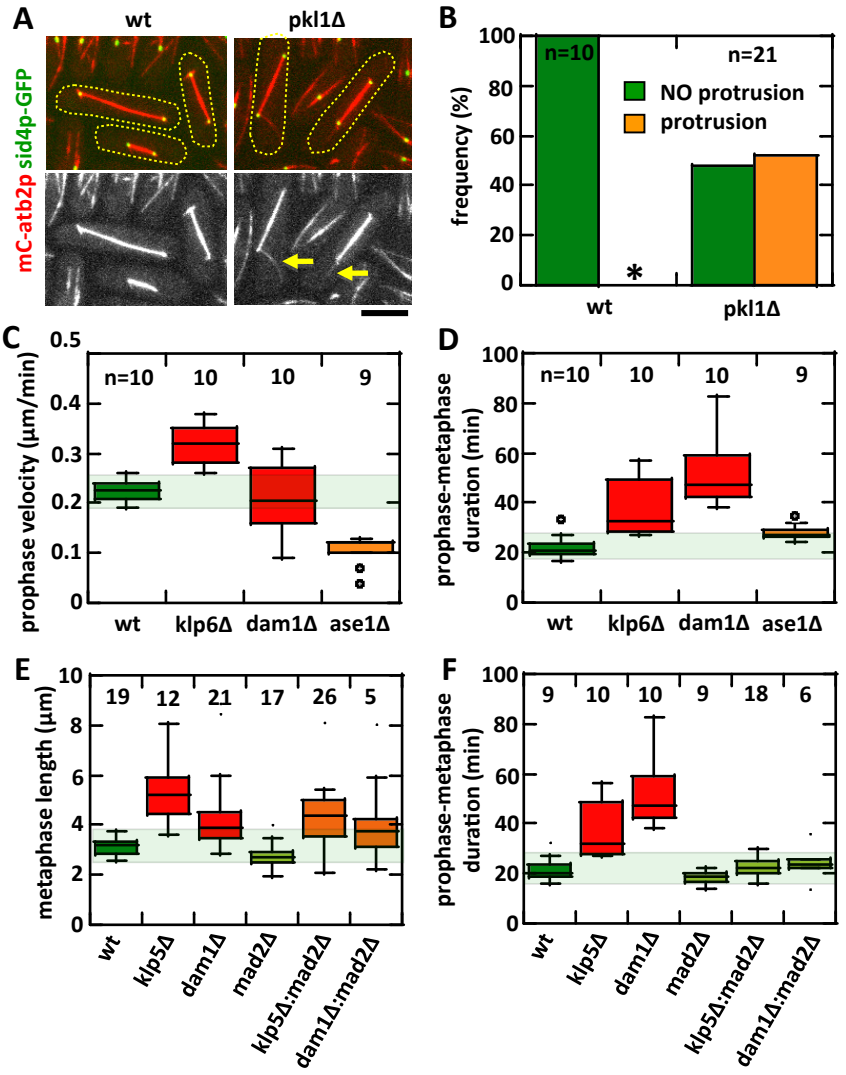

Figure S2. Syrovatkina et al.

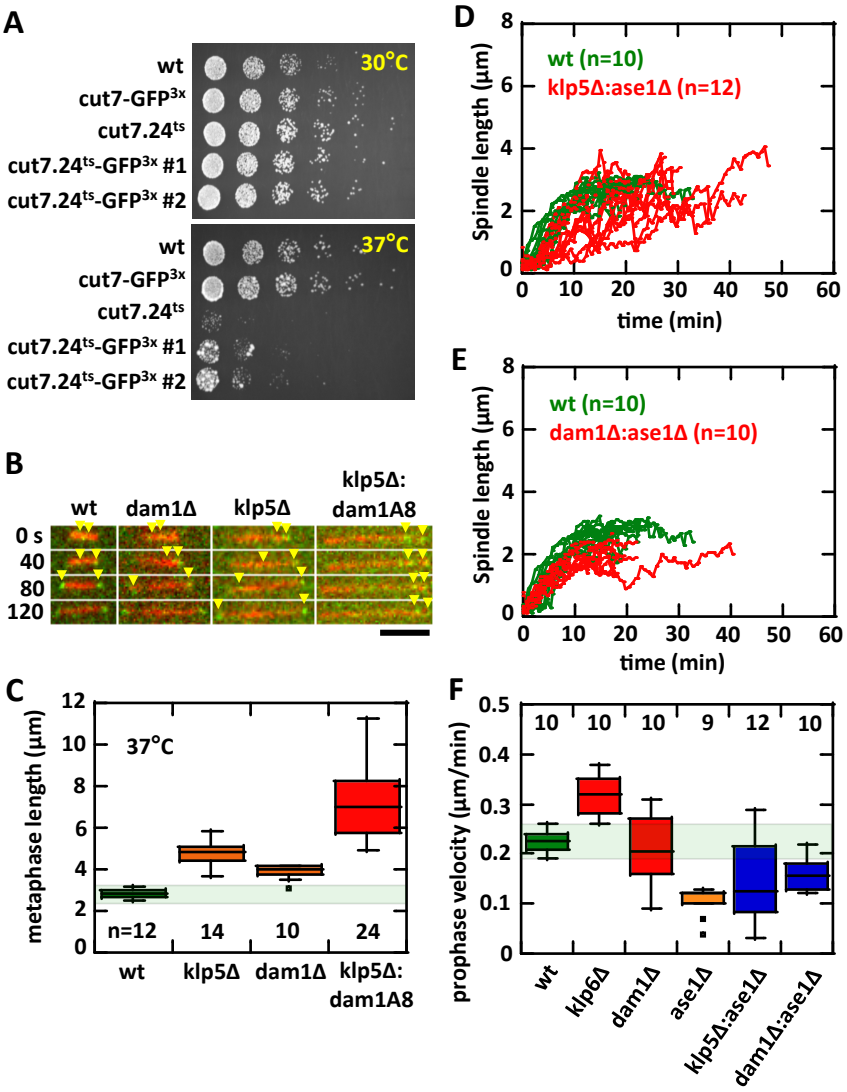

Figure S3. Syrovatkina et al.

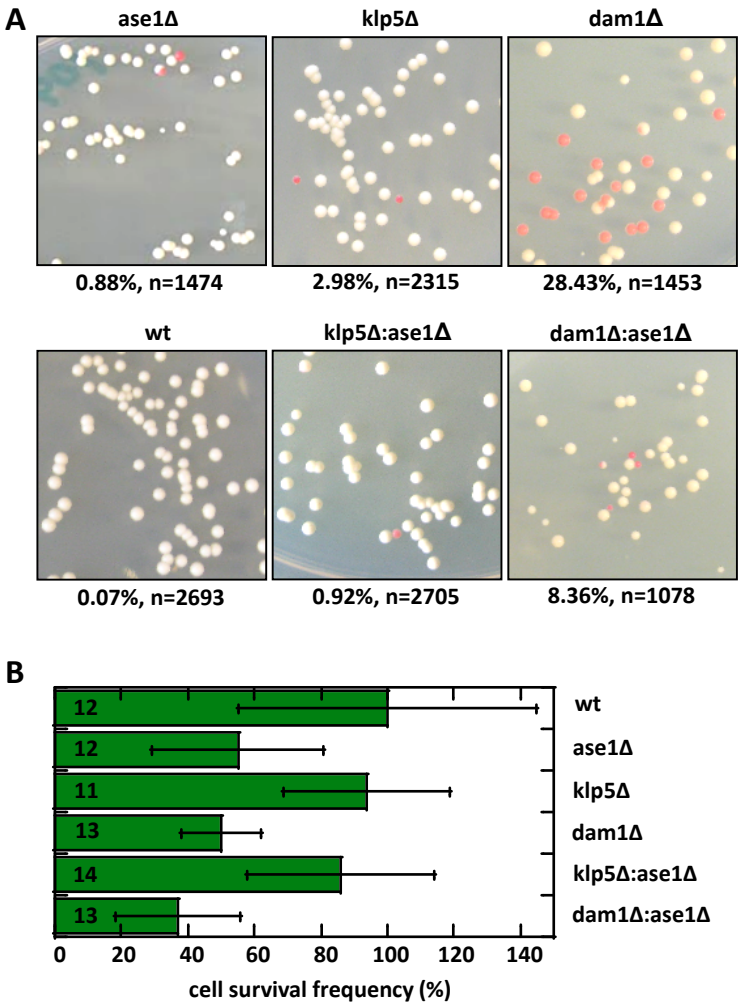

Figure S4. Syrovatkina et al.

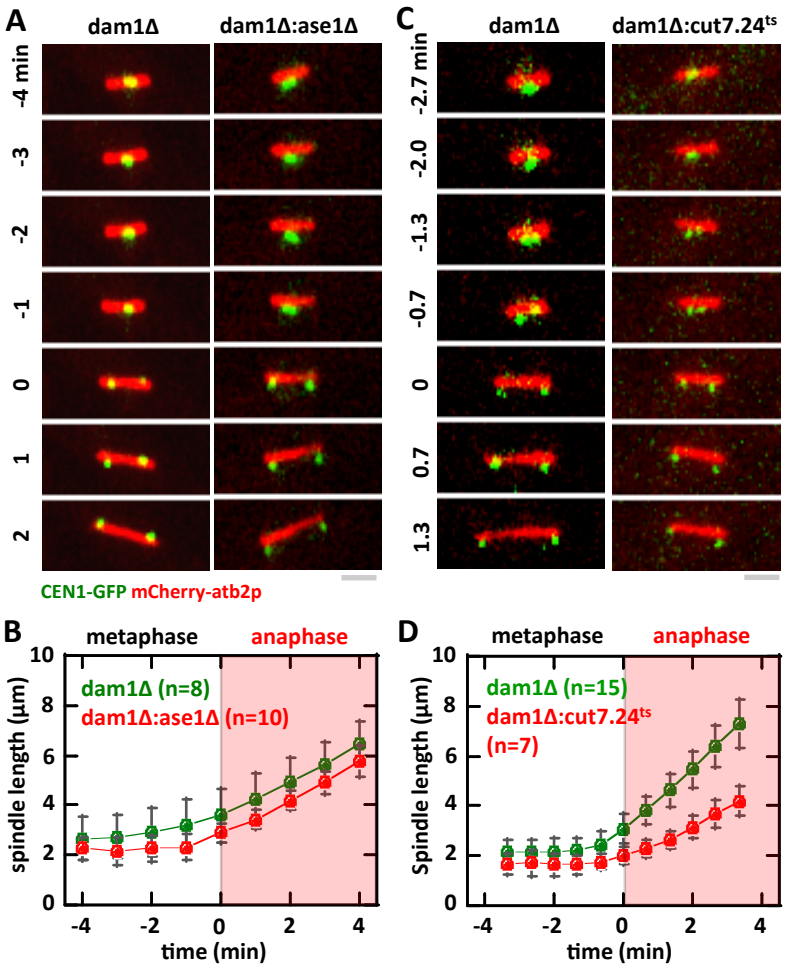

Figure Legends

Figure S1.

(A) Images of mitotic wildtype and pkl1Δ cells expressing mCherry-atb2p (tubulin) and sid4p-GFP (SPB marker). Wildtype mitotic cells show different spindles at different stages/lengths. Astral MTs are relatively short. In contrast, pkl1Δ cells have long astral MTs which protrude (yellow arrow) from the SPBs. Bar, 5 μm.

(B) Comparative plot of astral MT protrusion in wildtype and pkl1Δ cells. Where as wildtype cells show no astral MT protrusion, ~50% of pkl1Δ cells have astral MT protrusion, indicating spindle mal-formation [S1].

(C) Box plot of prophase velocities. Individual deletion klp6Δ and ase1Δ show different durations than wildtype. dam1Δ is similar to wildtype.

(D) Box plot of prophase-metaphase durations. Individual deletion klp6Δ, dam1Δ, and ase1Δ all show different durations than wildtype.

(E) Box plot of metaphase spindle lengths in response to the absence of the spindle assembly checkpoint proteins mad2p. Individual deletion mad2Δ resulted in similar metaphase spindle length compared to wildtype. In contrast, double-deletion klp5Δ:mad2Δ and dam1Δ:mad2Δ resulted in longer metaphase spindle lengths similar to klp5Δ and dam1Δ, respectively.

(F) Box plot shows prophase-metaphase duration in response to the absence of the spindle assembly checkpoint proteins mad2p. Individual mutants have prolonged prophase-metaphase durations compared to wildtype. In contrast, the double-mutants klp5Δ:mad2Δ and dam1Δ:mad2Δ have similar prophase-metaphase duration as wildtype.

Figure S2.

(A) Spot assay for temperature sensitivity of fission yeast strains: wildtype, cut7-GFP^{3x}, cut7.24^{ts}, cut7.24^{ts}-GFP^{3x} (1), and cut7.24^{ts}-GFP^{3x} (2). At permissive temperature 30°C, all strains survive well. In contrast, at the non-permissive temperature 37°C, cut7.24^{ts} is lethal [S2, S3]. However, when cut7.24^{ts} is tagged with GFP, the new strains survive slightly better than cut7.24^{ts} alone, suggesting that temperature-sensitivity is tenuous.

(B) Time-lapse images of wildtype, dam1Δ, klp5Δ and dam1-A8:klp5Δ mitotic cells expressing mCherry-atb2p (tubulin) and mis12p-GFP (kinetochore marker) at 37°C. Time 0 represents the transition from metaphase to anaphase A and anaphase B, where sister kinetochores (yellow arrow heads) are observed to separate to opposite poles, and the spindle elongates further. Note that the dam1-A8:klp5Δ failed to separate their kinetochores. Bar, 5 μm.

(C) Box plot of metaphase spindle lengths wildtype, dam1Δ, klp5Δ and dam1-A8:klp5Δ. Consistent with the force-balance or tug-of-war model, removal of individual dam1p or klp5p, which are passive and active inward force transducer, respectively, result in longer metaphase spindle lengths compared to wildtype. Further, inactivation of both dam1p and klp5p results in even longer metaphase spindle lengths compared to individual deletion.
(D) Comparative plot of spindle length versus time of wildtype (green) and klp5Δ:ase1Δ (red) cells. Similar to wildtype, klp5Δ:ase1Δ metaphase spindles plateau at ~3 μm length. However, the spindle elongation is unstable, varying from cell to cell.
(E) Comparative plot of spindle length versus time of wildtype (green) and dam1Δ:ase1Δ (red) cells. Similar to wildtype, dam1Δ:ase1Δ metaphase spindles plateau at ~3 μm length.
(F) Box plot of spindle prophase elongation velocities. Individual deletion klp6Δ, dam1Δ, and ase1Δ, as well as double-deletion klp5Δ:ase1Δ and dam1Δ:ase1Δ all show different velocities than wildtype.

Figure S3.
In an artificial mini-chromosome loss assay [S4], where cells which lose the artificial chromosome turn pink, we observed apparent rescue of chromosome segregation defects in double-deleted cells. Whereas wildtype has 0.07% of pink colonies, mutant ase1Δ has 0.88%, klp5Δ has 2.98%, and dam1Δ has 28.43% pink colonies (Fig. S3A), consistent with previous studies [S5-S7]. In contrast, klp5Δ:ase1Δ has 0.92% and dam1Δ:ase1Δ has 8.36% pink colonies, an apparent improvement in chromosome segregation (Fig. S3A). However, further analysis revealed that the mini-chromosome loss assay biases the results toward living cells, as dead cells cannot form colonies. Indeed, cell survival analysis revealed that wildtype and klp5Δ have similar ~100% survival rates, and mutant ase1Δ and dam1Δ have ~50% survival rate (Fig. S3B). Interestingly, while klp5Δ:ase1Δ has 86% survival rate, an improvement over ase1Δ alone, dam1Δ:ase1Δ has 37% survival rate, a significant decrease from dam1Δ alone (Fig. S3B). We thus conclude that rescuing spindle length by removing antagonistic forces can, in some cases, rescue chromosome segregation defects.
(A) Artificial mini-chromosome loss assays for wildtype and mutant cells. The double-deletion klp5Δ:ase1Δ and dam1Δ:ase1Δ appeared to have less chromosome loss than their respective single-deletion. However, this assay does not account for cell death on plates.
(B) Plot comparing cell survival on plates for the artificial mini-chromosome loss assays from Fig. S3A. Normalized wildtype cell survival is 100%. Individual deletion ase1Δ and dam1Δ have ~50% survival rate, while klp5Δ has similar survival rate as wildtype. Interestingly, the double-

deletion klp5Δ:ase1Δ appeared to have better survival rate than ase1Δ, but dam1Δ:ase1Δ has worse survival rate than either ase1Δ or dam1Δ.

Figure S4.

(A) Time-lapse images of dam1Δ and dam1Δ:ase1Δ mitotic cells expressing mCherry-atb2p and CEN1-GFP at 23°C. Time 0 represents the transition from metaphase to anaphase A where sister kinetochores are observed to separate to opposite poles. No spindle shrinkage prior to the metaphase to anaphase transition was observed. Bar, 1 μm.

(B) Comparative spindle length versus time plot of dam1Δ (green) and dam1Δ:ase1Δ (red) cells. Pole-to-pole distance was measured 4 minute before and 4 minutes after cells exhibit kinetochore separation to opposite poles. No spindle shrinkage prior to the metaphase to anaphase transition was observed.

(C) Time-lapse images of dam1Δ and dam1Δ:cut7.24^{ts} mitotic cells expressing mCherry-atb2p and CEN1-GFP at 37°C. Time 0 represents the transition from metaphase to anaphase A where sister kinetochores are observed to separate to opposite poles. No spindle shrinkage prior to the metaphase to anaphase transition was observed. Bar, 1 μm.

(D) Comparative spindle length versus time plot of dam1Δ (green) and dam1Δ:cut7.24^{ts} (red) cells. Pole-to-pole distance was measured 3.5 minute before and 3.5 minutes after cells exhibit kinetochore separation to opposite poles. No spindle shrinkage prior to the metaphase to anaphase transition was observed.

Table S1. List of *S. pombe* strains used in this study.

Strain	Genotype
PT.2133	cdc13-GFP:NatR mCherry-atb2:HygR leu1-32 URA4-D18 h-
CF.346	klp2Δ:URA4 cdc13-GFP:KanR mCherry-atb2:HygR ade6-m210? leu1-32 ura4.D18 his3.D1 h-
CF.348	klp3Δ:KanR cdc13-GFP:NatR mCherry-atb2:HygR ade6-m210? leu1-32 ura4-D18 h?
CF.349	tea2Δ:KanR cdc13-GFP:KanR mCherry-atb2:HygR ade6-m210? leu1-32 ura4-D18 h+
CF.350	klp5Δ:URA4 cdc13-GFP:KanR mCherry-atb2:HygR ade6-m210? leu1-32 ura4-D18 his3.D1 h-
CF.352	klp6Δ:URA4 cdc13-GFP:KanR mCherry-atb2:HygR ade6-m210? leu1-32 ura4-D18 his3.D1 h+
PT.3318	klp8Δ:NatR cdc13-GFP:KanR mCherry-atb2:HygR ade6-m210? leu1-32 ura4-D18 h+
CF.354	klp9Δ:KanR cdc13-GFP:KanR mCherry-atb2:HygR ade6-m210? leu1-32 ura4-D18 h?
CF.355	dhc1Δ:KanR cdc13-GFP:KanR mCherry-atb2:HygR ade6-m210? leu1-32 ura4-D18 h?
CF.356	ase1Δ:KanR cdc13-GFP:KanR mCherry-atb2:HygR ade6-m210? leu1-32? ura4-D18 h-
PT.2441	dam1Δ:KanR cdc13-GFP:NatR mCherry-atb2:HygR ade6-m210? leu1-32 ura4-D18 h-
CF.391	cut7.24 cdc13-GFP:NatR mCherry-atb2:HygR ade6-m210? leu1-32 ura4-D18 h+
CF.408	klp6Δ:URA4 cut7.24 cdc13-GFP:NatR mCherry-atb2:HygR ade6-m210? leu1-32 ura4-D18 h-
PT.2443	dam1Δ:KanR cut7.24 cdc13-GFP:NatR mCherry-atb2:HygR ade6-m210? leu1-32 ura4-D18 h-
PT.2210	ase1Δ:KanR klp5Δ:URA4 cdc13-GFP:NatR mCherry-atb2:HygR ade6-m210? leu1-32 h+
PT.2509	ase1Δ:KanR dam1Δ:KanR cdc13-GFP:NatR mCherry-atb2:HygR ade6-m210? leu1-32 ura4-D18 h-
CF.441	HIS7:LacI-GFP LYS1:LacO mCherry-atb2:HygR ade6-m210? leu1-32 ura4-D18 h+
PT.2887	klp5Δ:URA4 HIS7:LacI-GFP LYS1:LacO mCherry-atb2:HygR ade6-m210? leu1-32 ura4-D18 h+
CF.443	klp6Δ:URA4 HIS7:LacI-GFP LYS1:LacO mCherry-atb2:HygR ade6-m210? leu1-32 ura4-D18 h+
CF.445	dam1Δ:KanR HIS7:LacI-GFP LYS1:LacO mCherry-atb2:HygR ade6-m210? leu1-32 ura4-D18 h+
PT.2550	ase1Δ:KanR klp5Δ:URA4 HIS7:LacI-GFP LYS1:LacO mCherry-atb2:HygR ade6-m210? leu1-32 h?
PT.2698	ase1Δ:KanR dam1Δ:NatR HIS7:LacI-GFP LYS1:LacO mCherry-atb2:HygR ade6-m210? leu1-32 ura4-D18 h?
CF.474	klp6Δ:URA4 cut7.24 HIS7:LacI-GFP LYS1:LacO mCherry-atb2:HygR ade6-m210? leu1-32 ura4-D18 h+
PT.2815	dam1Δ:KanR cut7.24 HIS7:LacI-GFP LYS1:LacO mCherry-atb2:HygR ade6-m210? leu1-32 ura4-D18 h+
CF.658	miniChromosome Ch16:ADE6 ade6-210 his2 h+
PT.2626	ase1Δ:KanR miniChromosome Ch16:ADE6 ade6-210 his2 h?
PT.2639	klp5Δ:NatR miniChromosome Ch16:ADE6 ade6-210 his2 h?
PT.2637	dam1Δ:NatR miniChromosome Ch16:ADE6 ade6-210 his2 h?
PT.2552	klp5Δ:URA4 ase1Δ:KanR miniChromosome Ch16:ADE6 ade6-210 his2 h?
PT.2638	dam1Δ:NatR ase1Δ:KanR miniChromosome Ch16:ADE6 ade6-210 his2 h+
PT.3100	mad2Δ:KanR cdc13-GFP:NatR mCherry-atb2:HygR ade6-m210? leu1-32 ura4-D18 h+
PT.3102	klp5Δ:URA4 mad2Δ:KanR cdc13-GFP:NatR mCherry-atb2:HygR ade6-m210? leu1-32 ura4-D18 h+
PT.3122	dam1Δ:KanR mad2Δ:KanR cdc13-GFP:NatR mCherry-atb2:HygR ade6-m210? leu1-32 ura4-D18 h+
PT.3219	sid4-GFP:KanR mCherry-atb2:HygR leu1-32 ura4-D18 h-
PT.3280	pkl1Δ:NatR sid4-GFP:KanR mCherry-atb2:HygR ade6-m210? leu1-32 ura4-D18 h+
PT.1939	mCherry-atb2:HygR leu1-32 URA4-D18 h-
PT.2973	cut7-3xGFP mCherry-atb2:HygR ade6-m210? leu1-32 ura4-D18 h-
CF.340	cut7.24 mCherry-atb2:HygR ade6-m210? leu1-32 ura4-D18 h-
PT.3315	cut7.24-3xGFP mCherry-atb2:HygR ade6-m210? leu1-32 ura4-D18 h+ (1)
PT.3316	cut7.24-3xGFP mCherry-atb2:HygR ade6-m210? leu1-32 ura4-D18 h+ (2)
CF.124	mis12-GFP:LEU2 mCherry-atb2:HygR leu1-32 h-
PT.2441	dam1Δ:NatR Mis12-GFP:LEU2 mCherry-atb2:HygR leu1-32 h+
PT.3407	klp5Δ:URA4 Mis12-GFP:LEU2 mCherry-atb2:HygR leu1-32 h+
PT.3328	dam1-A8-GFP:NatR klp5Δ:URA4 Mis12-GFP:LEU2 mCherry-atb2:HygR leu1-32 h+

Experimental Procedures

Strains and media

Standard fission yeast media and techniques were used as described [S8]. Deletions were constructed by an established homologous recombination technique [S9]. Strains used in this study are listed in Table S1.

Microscopy

Yeast cells were imaged with a Yokogawa spinning-disc confocal microscope equipped with Nikon PlanApo 100X/1.45 NA objective lens and a Hamamatsu cooled back-thinned CCD-camera or EM-CCD camera as previously described [S10]. Images were acquired and processed with MetaMorph 7.7 (www.MolecularDevices.com). For experiments involving cut7.24^{ts} temperature shift, cells were first imaged at room temperature of 23°C then shifted to the non-permissive temperature of 35°C by either the fast microfluidic temperature device [S11], or 37°C by a home-built fast temperature box. To precisely indentify the transition from metaphase to anaphase, cdc13p-GFP signal disappearance from the spindle was used [S12]. Additional details of imaging conditions are provided for each figure in supplemental section.

Data Analysis

Spindle lengths were measured by calculating pole-to-pole distances, whose x-y positions were automatically tracked by MTtrackJ plugin in ImageJ (www.imagej.gov) for Fig. 1D-F and 2D-E. Data were plotted as box plots generated with Kaleidagraph 4.0 (www.synergy.com). Each box encloses 50% of the data with the median value displayed as a line. The top and bottom of each box mark the minimum and maximum values within the data set that fall within an acceptable range. Any value outside of this range, called an outlier, is displayed as an individual point. Statistical analyses of data were performed using the Student's t-test for comparison between means, or Chi-squared test for comparison between frequencies in Microsoft Excel 2010.

Imaging

The precise live-cell imaging conditions are stated below for each figure.

Fig. 1A, S1A, 3A, 4A, S4A: 3D timelapse stacks consisting of 11 optical sections of 0.5 µm spacing were collected every 1 min with 600-ms exposure for GFP and 800-ms exposure for mCherry.

Fig. 1C, 2A, 2B, 2C: Images were acquired every 1 min with 1000-ms exposure for both GFP and mCherry. Cell chambers were switched from 23°C (blue) to 35°C (red) with a microfluidic temperature control device.
Fig. S2B: Images were acquired every 40 sec with 1000-ms exposure for both GFP and mCherry. Cell chambers were switched from 23°C (blue) to 37°C (red) with a temperature control device.
Fig. 4C, S4C: 3D timelapse stacks consisting of 11 optical sections of 0.5 μm spacing were collected every 40 sec with 600-ms exposure for GFP and 800-ms exposure for mCherry.

Minichromosome loss assay

The assay was performed as previously described [S4]. Briefly, cells (600 cells based on OD measurements) containing the artificial mini-chromosome were plated onto selection plates YE4S and incubated at 30°C for 3 days. Total colonies and pink colonies were counted to provide cell survival frequencies and percentage of chromosome loss.

Spot assay

For all strains, initial cell concentrations were normalized to OD=0.5. For each strain, successive dilutions of 1, 10^{-1}, 10^{-2}, 10^{-3}, 10^{-4}, 10^{-5} were spotted at 3 μL onto YE5S plates. Plates were incubated for 3 days at 30°C (control, permissive temperature) or at 37°C (test, non-permissive temperature).

References

S1. Troxell, C.L., Sweezy, M.A., West, R.R., Reed, K.D., Carson, B.D., Pidoux, A.L., Cande, W.Z., and McIntosh, J.R. (2001). pkl1(+)and klp2(+): Two kinesins of the Kar3 subfamily in fission yeast perform different functions in both mitosis and meiosis. Molecular biology of the cell *12*, 3476-3488.

S2. Hagan, I., and Yanagida, M. (1990). Novel potential mitotic motor protein encoded by the fission yeast cut7+ gene. Nature *347*, 563-566.

S3. Hagan, I., and Yanagida, M. (1992). Kinesin-related cut7 protein associates with mitotic and meiotic spindles in fission yeast. Nature *356*, 74-76.

S4. Niwa, O., Matsumoto, T., Chikashige, Y., and Yanagida, M. (1989). Characterization of Schizosaccharomyces pombe minichromosome deletion derivatives and a functional allocation of their centromere. The EMBO journal *8*, 3045-3052.

S5. Sanchez-Perez, I., Renwick, S.J., Crawley, K., Karig, I., Buck, V., Meadows, J.C., Franco-Sanchez, A., Fleig, U., Toda, T., and Millar, J.B. (2005). The DASH complex and Klp5/Klp6 kinesin coordinate bipolar chromosome attachment in fission yeast. The EMBO journal *24*, 2931-2943.

S6. West, R.R., Malmstrom, T., and McIntosh, J.R. (2002). Kinesins klp5(+) and klp6(+) are required for normal chromosome movement in mitosis. Journal of cell science *115*, 931-940.

S7. Yamashita, A., Sato, M., Fujita, A., Yamamoto, M., and Toda, T. (2005). The roles of fission yeast ase1 in mitotic cell division, meiotic nuclear oscillation, and cytokinesis checkpoint signaling. Molecular biology of the cell *16*, 1378-1395.

S8. Moreno, S., Klar, A., and Nurse, P. (1991). Molecular genetic analysis of fission yeast Schizosaccharomyces pombe. Methods in enzymology *194*, 795-823.

S9. Bahler, J., Wu, J.Q., Longtine, M.S., Shah, N.G., McKenzie, A., 3rd, Steever, A.B., Wach, A., Philippsen, P., and Pringle, J.R. (1998). Heterologous modules for efficient and versatile PCR-based gene targeting in Schizosaccharomyces pombe. Yeast *14*, 943-951.

S10. Tran, P.T., Paoletti, A., and Chang, F. (2004). Imaging green fluorescent protein fusions in living fission yeast cells. Methods *33*, 220-225.

S11. Velve Casquillas, G., Fu, C., Le Berre, M., Cramer, J., Meance, S., Plecis, A., Baigl, D., Greffet, J.J., Chen, Y., Piel, M., et al. (2011). Fast microfluidic temperature control for high resolution live cell imaging. Lab Chip *11*, 484-489.

S12. Fu, C., Ward, J.J., Loiodice, I., Velve-Casquillas, G., Nedelec, F.J., and Tran, P.T. (2009). Phospho-regulated interaction between kinesin-6 Klp9p and microtubule bundler Ase1p promotes spindle elongation. Developmental cell *17*, 257-267.